JOURNAL OF ELECTROMAGNETIC ENGINEERING AND SCIENCE, VOL. 22, NO. 6, 665~677, NOV. 2022

https://doi.org/10.26866/jees.2022.6.r.136
ISSN 2671-7263 (Online) · ISSN 2671-7255 (Print)

An Efficient Cross-Correlation Method for a Digital Phase Noise Measurement System

Kyung-Whan Yeom* · Jin-Seong Roh

Abstract

In this paper, we propose a digital phase noise measurement using a 10-bit digital oscilloscope MXR608A from Keysight Technologies. The digital oscilloscope's four channel data are used for digital phase noise measurement: two channels are assigned for the equally divided SUT (source under test), while the other two are assigned for the equally divided reference signals. First, we propose a cross correlation method to identify the phase noises added by the ADCs in the digital oscilloscope from the measured phase noises. Then, we propose a novel cross correlation method to extract the SUT phase noise. The cross-correlation output of the proposed method yields only the SUT phase noise and does not contain the reference signal phase noise unlike the traditional method. The proposed method was applied to measure the phase noises of the two SUTs, Keysight's synthesized signal generator E8257D and function generator 33600A. The measured phase noises of the two SUTs were compared and found to show remarkable agreements with those measured using Keysight's signal source analyzer E5052B. The phase noise floor of our digital phase noise measurement system is about −160 dBc/Hz.

Key Words: Cross Correlation, Digital Phase Noise Measurement, Phase Noise, Phase Noise Measurement.

I. Introduction

Phase noise is the frequency-domain representation of a random fluctuation in the phase of a waveform. More precisely, it is defined according to the IEEE [1] as

$$L(f_m) = \frac{P_n}{P_s} \tag{1}$$

where P_s, P_n, and f_m represent the total signal power, the power density in one phase noise modulation sideband per Hz, and the offset frequency, respectively. When constructing a communication system, the phase noise performance of a source is generally an important specification that must be considered [2–4]. However, accurate phase noise measurement remains an extremely challenging task.

Analog phase noise measurement methods can be classified into three: direct spectrum method, frequency discriminator method, and phase detector method [5, 6]. The direct spectrum method, the simplest method for measuring phase noise, uses a spectrum analyzer [5]. This method is unsuitable for measuring oscillators with ultra-low phase noise performance, as the noise floor of the instrument is comparatively high. In the frequency discriminator method, the frequency fluctuations of a signal are translated to low-frequency voltage fluctuations that can then be measured using a baseband analyzer. The phase noise is thus measured from the frequency fluctuations. This method is suitable for free running oscillators, such as LC oscillators or cavity oscillators [5].

In the phase detector method [5, 6], the most widespread

Manuscript received March 28, 2022 ; Revised June 2, 2022 ; Accepted June 28, 2022. (ID No. 20220328-042J)
Department of Radio Science and Engineering, Chungnam National University, Daejeon, Korea.
*Corresponding Author: Kyung-Whan Yeom (e-mail: khyeom@cnu.ac.kr)

method for measuring phase noise, a voltage-controlled oscillator with a low phase noise is necessary for the reference source, which is phase locked to an SUT (source under test) using a narrowband feedback loop. In the locked state, the reference source has the same frequency as the SUT and maintains a phase quadrature. The phase detector detects the phase difference of the SUT from the reference source, which corresponds to the phase noise. The phase detector method can measure extremely low phase noise with a good reference source. Using two-channel correlation, the phase noise floor of the phase detector method can be further improved: it can be further lowered by about 20 dB [5]. Today, combining the previous methods, state-of-the-art phase noise measurement equipment—that shows a phase noise floor close to −180 dBc/Hz at a far-out offset frequency of >1 MHz [7, 8]—is available on the market.

Digital phase noise measurement systems began gaining interest for their suitability as a cheap automatic test equipment in mass-production tests [9]. In a digital phase noise measurement system, the SUT signal is digitally sampled, and its phase is detected using a digital quadrature demodulator. A simple fast Fourier transform (FFT) operation on the SUT's detected phase results in the phase noise. However, the phase noise floor of digital phase noise measurement systems is generally quite higher than that of the best analog phase noise measurement system. Furthermore, the frequency range of the digital phase noise measurement system is basically limited to low frequencies of about tens of MHz range.

Significant improvement in the phase noise floor of the digital phase noise measurement systems can be achieved by removing the ADC clock jitter noise [10]. The work in [10] used four identical ADCs characterized by 14 bits or more, and the two-channel cross correlation technique was applied to suppress the ADC noise after the ADC clock jitter removal. The work, implemented using FPGAs and DSPs, achieved a phase noise floor of about −170 dBc/Hz. However, the SUT frequency range of the work is still limited to the frequency range of 1–30 MHz. Due to the low-frequency range, it must be used in conjunction with a down converter to measure the phase noise of SUTs at higher frequencies. Several studies have been conducted to extend digital phase noise measurement systems to higher frequencies using subsampling or downconverters [11–13].

In this study, we aimed to measure phase noise using a digital oscilloscope. It offers easier hardware implementation than FPGA and DSP implementation for a digital phase noise measurement system. Moreover, it may allow the realization of cheap automatic solutions that can be released as a software option. Furthermore, the ADCs in the digital oscilloscope usually have a wide bandwidth up to several gigahertz, and the phase noise of a high frequency SUT for communication systems can be measured without external downconverters. However, a digital oscilloscope has nominally a 10-bit resolution, which inevitably results in poor phase noise floor. The phase noise sensitivity using the digital oscilloscope is usually poor and is above −110 dBc/Hz [14]. In this paper, we provide a digital noise measurement system using a 10-bit digital oscilloscope with a phase noise sensitivity of about −160 dBc/Hz.

Second, we present a novel analysis of the measured phase noise. As a result, the ADC clock jitter noise and the thermal phase noise floor—the phase noises added by an ADC—can be identified. The analysis leads to the novel cross correlation method capable of extracting the true SUT phase noise alone. Consequently, the true SUT phase noise can be obtained by removing the phase noises added by the ADC. In addition, the proposed method, unlike the previous works, does not need a reference signal whose phase noise is low enough compared to the SUT phase noise. The proposed method alleviates the choice of the reference source, and the optimal reference source frequency can be freely selected. In this paper, under the previously explained motivation, we present a novel phase noise measurement method using the digital oscilloscope MXR608A [15] from Keysight Technologies.

II. Phase Noise Measurement System

1. Configuration

Fig. 1 shows our phase noise measurement system configuration. The analog time domain signals $s(t)$ and $s_{REF}(t)$ in Fig. 1 represent the SUT and reference signals. The four ADCs represent the four channels of the digital oscilloscope

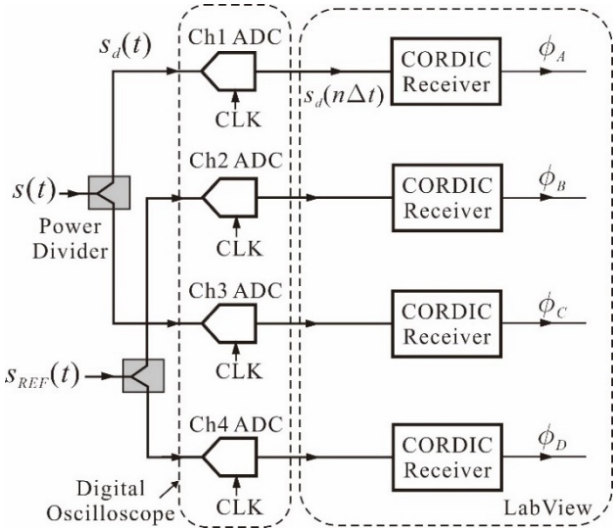

Fig. 1. Phase noise measurement system. The analog time domain signals $s(t)$ and $s_{REF}(t)$ represent the SUT and reference signals. The four ADCs represent four channels of the digital oscilloscope. Using the LabView program from National Instruments, the sampled channel data are read into the PC and their phases ϕ_A, ϕ_B, ϕ_C, and ϕ_D are detected.

MXR608A from Keysight Technologies. The two power dividers, ZFRSC-183−S+ from Mini Circuits, divide $s(t)$ and $s_{REF}(t)$. The divided $s(t)$ and $s_{REF}(t)$ are applied to channels 1, 3 and 2, and 4 of the digital oscilloscope, respectively, and they are sampled at every Δt. The sampling frequency f_s is thus $(\Delta t)^{-1}$.

The USB device port of MXR608A is connected to the host PC. The sampled channel data is first stored in the memory of MXR608A, and the stored data is read into the PC using the LabView of National Instruments. The length N_L of the sampled channel data that can be read into a PC is limited by both the memory size and the Labview data processing capacity. In our setup, N_L is limited by the LabView data processing capacity, and the maximum N_L is about 4M samples. Both N_L and f_s determines the frequency range and resolution of the Fourier transform of the data read into PC. The frequency range is given by $\frac{1}{2}f_s$, while the frequency resolution or the frequency spacing Δf is determined by $\Delta f = f_s/N_L$. The frequency resolution also becomes the lowest frequency of the Fourier transform. Therefore, the phase noise below Δf cannot be measured.

Fig. 2 shows the detailed CORDIC (coordinate rotation digital computer) [16, 17] receiver in Fig. 1. The CORDIC receiver is implemented using LabView and it detects the phase of the data read into the PC. The digital-down converters (DDC) is a multiplier that takes the product of two waveforms. The ω of $s_d(n\Delta t)$ was detected using *Extract Single Tone Information.vi* (virtual instrument) of LabView. The orthogonal LO signals $\cos\{\omega(n\Delta t)\}$ and $\sin\{\omega(n\Delta t)\}$, where ω is equal to that of $s_d(n\Delta t)$ were generated using *Sine Waveform.vi* of LabView. The two DDCs produce $\cos\phi$ and $\sin\phi$. The phase ϕ is obtained by taking the $\tan^{-1}$ operation. In FPGA programming, ϕ is obtained from $\cos\phi$ and $\sin\phi$ by iterative calculation using the CORDIC algorithm. However, in LabView implementation, ϕ is simply obtained using a $\tan^{-1}$ operation, and implementing the CORDIC algorithm is unnecessary.

At the DDC output, the second harmonic appears. In addition, since $\cos\phi$ and $\sin\phi$ change slowly, the decimation of the higher input sample rate is necessary. The lowpass filter (LPF) in Fig. 2 both removes the second harmonic and decimates the input sample rate. The digital infinite impulse response (IIR) elliptic LPF is then added for the second harmonic rejection. After the digital IIR elliptic LPF, decimation is achieved using *Waveform Resample.vi* of LabView. Fig. 3 demonstrates the phase noise measurement system.

2. Phase Spectrum

In Fig. 2, ϕ is a time domain signal, and the phase spectrum $S_\phi(f_m)$ [1] can be obtained from the power spectral density (PSD) of ϕ. Finally, the phase noise $L(f_m)$ in (1) can be obtained from $S_\phi(f_m)$ as

$$L(f_m) = \frac{1}{2}S_\phi(f_m). \tag{2}$$

The cross-power spectrum for the two selected phase fluctuations from ϕ_A, ϕ_B, ϕ_C, and ϕ_D in Fig. 1 is frequently necessary to obtain the phase noise. The cross-power spectrum is obtained using the *Cross Spectrum (Real-Im).vi* in LabView. The cross-power spectrum of two random signals results in a complex number in the frequency domain, one having real and imaginary parts. Moreover, in this paper, the cross-power spectral density of ϕ_A and ϕ_B and its real and imaginary parts are denoted as $X(\phi_B, \phi_B; f_m) = R_{AB} + jI_{AB}$. Thus, $X(\phi_B, \phi_B; f_m)$ is

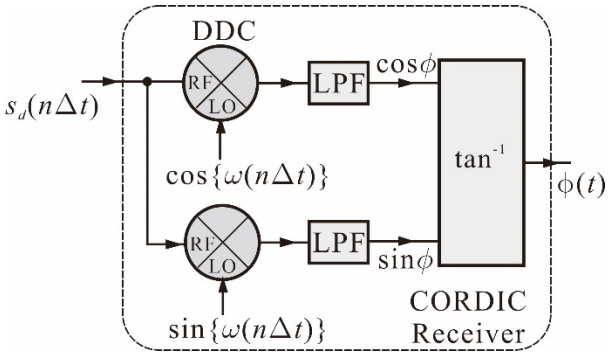

Fig. 2. The configuration of the CORDIC receiver in Fig. 1. The DDC is a digital multiplier and its LO frequency ω is equal to that of $s_d(n\Delta t)$. The LPF filters out the second harmonic appearing at the output of the DDC and decimates appropriately the input sampling rate at the same time. The phase ϕ is obtained through $\tan^{-1}$ operation from $\cos\phi$ and $\sin\phi$.

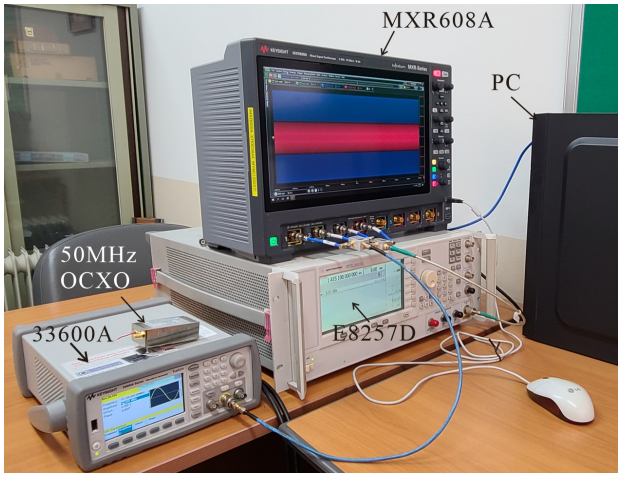

Fig. 3. Photograph of the measurement setup. The USB device port of the digital oscilloscope MXR608A is connected to the USB port of the host PC.

$$X(\phi_A, \phi_B; f_m) = R_{AB} + jI_{AB} = \frac{\overline{F(\phi_A)}F(\phi_B)}{w \cdot \Delta f}. \quad (3)$$

In Eq. (3), $F(\cdot)$ represents the Fourier transform, and the top bar of $F(\cdot)$ the complex conjugate of the Fourier transform. Δf represents bandwidth, and w the equivalent noise bandwidth (ENBW) of window function. The real part R_{AB} corresponds to the power spectrum due to the correlated parts of two random signals, while the imaginary part I_{AB} represents the power spectrum due to the uncorrelated parts. R_{AB} converges to a finite value, while I_{AB} converges to zero as the average number of the cross-power spectrum increases.

The selected window in Eq. (3) is a seven-term Blackman Harris window and $w = 2.63191$. The spectral leakage of the four-term Blackman Harris window is known to be below about -90 dB. Taking the dynamic range of phase noise measurement into consideration, -90 dB may not be enough, and the seven-term Blackman Harris window, which yields a spectral leakage of about -150 dB, is selected [18].

Phase noise $L(f_m)$ is usually plotted on a log scale f_m. However, $S_\phi(f_m)$ is usually computed from equidistant time domain samples. As a result, $S_\phi(f_m)$ is uniformly spaced on fm defined over $[f_{start}, f_{stop}]$. When $S_\phi(f_m)$ is plotted on a log scale fm, it is densely spaced at a higher f_m, which results in higher fluctuation. The way to reduce the fluctuation of $S_\phi(f_m)$ at higher f_m is to increase its average number, particularly at a higher f_m. Since the average number of $S_\phi(f_m)$ increases as f_m increases, the successively decimating FFT structure [19] is efficient for reducing the fluctuation of $S_\phi(f_m)$ at higher f_m. This structure is appropriate for FPGA implementation.

However, instead of using the successively decimating FFT structure, the fluctuation at higher f_m can be efficiently reduced by increasing the averaging bandwidth as f_m increases. Instead of linearly spaced f_m defined over $[f_{start}, f_{stop}]$, a new set of log-spaced offset frequency, $f_{m,\log}(n)$ can be defined on $[f_{start}, f_{stop}]$. The n-th element of log-spaced offset frequency $f_{m,\log}(n) = f_{start}10^{kn}$ for a constant k and $n = 0, \cdots, N$, where N is the number of log-spaced offset frequencies. For a newly defined log-spaced $f_{m,\log}$, the bandwidth BW can be defined to increase with $f_{m,\log}$ as

$$BW = \frac{f_{m,\log}(n)}{Q} \quad (4)$$

where Q is constant, specifying the number of uniformly spaced spectrums to be included for averaging at $f_{m,\log}(n)$. Now, the value of $S_\phi(f_{m,\log})$ can be computed as the average of the spectrums $S_\phi(f_m)$ within BW. Consequently, $S_\phi(f_{m,\log})$ will show the reduced fluctuation at higher $f_{m,\log}$. Similar spectral estimation methods can be found in [20] and [21]. We named this the logarithmic bandwidth averaging (LBA), which is more efficient in LabView programming than the successively decimating FFT structure. The LBA is programmed using MATLAB and implemented using the *MATLAB Script Node.vi* in LabView.

III. ADC Phase Noises

The time domain phase fluctuations ϕ_A, ϕ_B, ϕ_C, and ϕ_D in Fig. 1 can be modeled simply by the sum of the phase fluctuations as follows:

$$\phi_A = \phi_d + a\phi_c + \phi_1 \quad (5a)$$

$$\phi_B = \phi_{ref} + b\phi_c + \phi_2 \quad (5b)$$

$$\phi_C = \phi_d + a\phi_c + \phi_3 \quad (5c)$$

$$\phi_D = \phi_{ref} + b\phi_c + \phi_4. \quad (5d)$$

In Eq. (5), ϕ_d and ϕ_{ref} represent the SUT and reference signal phase fluctuations, while ϕ_c represents the phase fluctuation due to the ADC clock jitter. The constants a and b represent the scaling constants of the phase fluctuation due to the ADC clock jitter. Since the frequencies of the SUT and reference signal are generally different, the phase fluctuation due to the ADC clock jitter differs, as in Eqs. (5a) and (5b). The ϕ_1, ϕ_2, ϕ_3, and ϕ_4 represent the phase fluctuations originating from the quantization and thermal noises of the ADCs, which are almost white in the frequency domain. In addition, ϕ_1, ϕ_2, ϕ_3, and ϕ_4 are uncorrelated.

1. ADC Phase Noise Floor

The phase fluctuations ϕ_1, ϕ_2, ϕ_3, and ϕ_4 in Eq. (5) due to the ADC noises correspond to the phase noise floor for the digital phase noise measurement. Usually, instead of ADC phase fluctuations like ϕ_j ($j = 1, 2, 3$, or 4), ADC performance is characterized by signal-to-noise ratio (SNR). The ADC SNR is given by [22] as follows:

$$\text{SNR(dB)} = 6.02B + 1.76 + 10\log(f_s) - 3 \quad (6)$$

where B is the number of bits of the ADC, and f_s is the sampling frequency (or sampling rate). The SNR in Eq. (6) can be used to estimate the measurable phase noise range at a higher f_m because $L(f_m)$ in Eq. (1) can be interpreted as SNR. Thus, the SNR in Eq. (6) corresponds to the phase noise floor. In the case of the 10-bit digital oscilloscope, the value of the SNR is computed to be about -140 dBc/Hz for a sampling frequency of $f_s = 100$ MHz. However, the real ADCs are imperfect and introduce additional noise and distortion. The SNR estimation by Eq. (6) shows a significant gap from the real SNR. The concept of the effective number of bits (ENOB) was introduced based on the measured SNR or SINAD. However, even the ENOB is not a true phase noise floor. In this paper, we propose

the measurement method of the true phase noise floor $P_{\phi_j}(f_s)$ due to ϕ_j ($j = 1$, 2, 3, and 4) in Eq. (5) using the cross-correlation. The true phase noise floor $P_{\phi_j}(f_s)$ can be computed from the phase spectrum of $S_{\phi_j}(f_m)$ as $P_{\phi_j}(f_s) = \frac{1}{2}S_{\phi_j}(f_m)$ and is only the function of the sampling frequency f_s.

In Eq. (5), the correlated part between $(\phi_A - \phi_C)$ and ϕ_A is only ϕ_1. Similarly, the correlated part between $(\phi_A - \phi_C)$ and ϕ_C is only ϕ_3. Therefore, $S_{\phi_1}(f_m)$ and $S_{\phi_3}(f_m)$ are given by

$$S_{\phi_1}(f_m) = \langle X(\phi_A - \phi_C, \phi_A; f_m)\rangle_{M\to\infty} \tag{7a}$$

$$S_{\phi_3}(f_m) = \langle X(\phi_A - \phi_C, \phi_C; f_m)\rangle_{M\to\infty}. \tag{7b}$$

Here, $\langle\cdot\rangle$ represents the average operation and M is the average number. Now, the phase noise floors due to ϕ_1 and ϕ_3 are determined as $P_{\phi_1}(f_s) = \frac{1}{2}S_{\phi_1}(f_m)$ and $P_{\phi_3}(f_s) = \frac{1}{2}S_{\phi_3}(f_m)$ from Eq. (7). Similarly, the phase noise floors due to ϕ_2 and ϕ_4 can be obtained. The measured phase noise floor $P_{\phi_1}(f_s)$ due to ϕ_1 is shown in Fig. 4. The average number M of the cross-power spectrum is set to $M = 50$. The effects of ϕ_d and ϕ_c on $S_{\phi_1}(f_m)$ in Eq. (7a) are significant at lower f_m, while their effects at higher f_m rapidly decrease and become smaller. As a result, $S_{\phi_1}(f_m)$ at a lower f_m shows a significant fluctuation, while $S_{\phi_1}(f_m)$ at a higher f_m converges to the phase noise floor value as shown in Fig. 4. Therefore, the phase noise floor values can be found by reading their values at a far-out offset frequency.

The measured phase noise floor values in Fig. 4 for $f_s = 1$, 4, 16 GHz are about −128 dBc/Hz, −134 dBc/Hz, and −139 dBc/Hz (about −150 dBc/Hz, −156 dBc/Hz, and −162 dBc/Hz by Eq. (6)), respectively. As expected, the phase noise floor value predicted by Eq. (6) shows a significant gap. Since the digital oscilloscope has a 10-bit resolution, the phase noise floor is poor, as shown in Fig. 4, even though f_s is set to several gigahertz. As f_s increases, the phase noise floor is lowered and is about 6 dB down per one octave increase in f_s. The measured $P_{\phi_j}(f_s)$ ($j = 1$, 2, 3, and 4) are almost equal. Thus, the phase noise floors at f_s are denoted by $P_{\phi_1}(f_s) = P_{\phi_2}(f_s) = P_{\phi_3}(f_s) = P_{\phi_4}(f_s) = P_{\phi}(f_s)$.

The phase noise floor limits the practically measurable phase noise range of an SUT. To simplify the explanation, we assume that the phase fluctuation due to ADC clock jitter is 0. In this case, $\phi_c = 0$ for ϕ_A and ϕ_C in Eqs. (5a) and (5c). Under the assumption, the SUT phase noise $S_{\phi_d}(f_m)$ can be obtained from $\langle X(\phi_A, \phi_C; f_m)\rangle_{M\to\infty}$. Note that the $X(\phi_A, \phi_C; f_m)$ includes the cross-power spectrums of the uncorrelated terms as well as $S_{\phi_d}(f_m)$. As $M\to\infty$, the cross-power spectrums of the uncorrelated terms converge to 0, and $S_{\phi_d}(f_m)$ can be obtained. Therefore, the cross-power spectrums of the uncorrelated terms in $X(\phi_A, \phi_C; f_m)$ become the phase noise floor. It is known that the cross-power spectrum of two uncorrelated signals decreases by about 5 dB per a decade increase of M [23]. However, it is impossible to increase the average number $M\to\infty$. The time necessary for the cross-power spectrum average number $M = 10{,}000$ is about a day for a PC with a 3.6 GHz Intel i3 CPU and a RAM of 64 GB. We take the time necessary for the average number $M = 10{,}000$ as the practical time limit for the phase noise measurement. Therefore, the phase noise floor improvement using the cross-correlation technique is practically limited by 20 dB.

Under the assumption $\phi_c = 0$, the phase noise floor for the cross-power spectrum $X(\phi_A, \phi_C; f_m)$ is determined by $X(\phi_1, \phi_3; f_m)$, which decreases with M as follows:

$$\langle X(\phi_1, \phi_3; f_m)\rangle_M \approx \sqrt{\frac{1}{M}}P_{\phi}(f_s). \tag{8}$$

Since $P_{\phi}(f_s)$ in Fig. 4 is about −128 dBc/Hz at a sampling frequency of $f_s = 1$ GHz, $\langle X(\phi_1, \phi_3; f_m)\rangle_M = 10{,}000$ will be about −148 dBc/Hz. To decrease the phase noise floor further by 10 dB more requires a time of about 100 days, which is intolerable and impossible. Therefore, the phase noise of about −148 dBc/Hz for $f_s = 1$ GHz is the limit value that can be measured using this setup. The SUT with the phase noise above −148 dBc/Hz at far-out offset frequencies can be measured, but the phase noise below −148 dBc/Hz cannot be measured. From Fig. 4, the measurable phase noise range for $f_s = 16$ GHz is estimated to be about −160 dBc/Hz.

Lower phase noise can be measured by increasing the sampling frequency f_s. However, to measure the phase noise at a lower offset frequency f_m, the length of the sampled data N_L should be increased in proportion to the increase in f_s. The minimum offset frequency $f_{m,min}$ for a given sample data length N_L is determined by

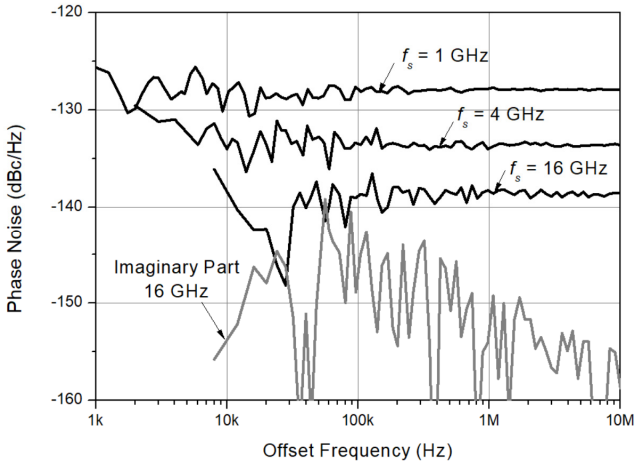

Fig. 4. The measured phase noise floor of ϕ_1. The average number of the cross spectrums is $M = 50$. The measured phase noise floors of ϕ_2, ϕ_3, and ϕ_4 are within ± 1 dB.

$$f_{m,min} = \frac{f_s}{N_L}. \tag{9}$$

As explained in Section II-1, the sample data length N_L cannot be increased without limit due to the LabView data processing capacity. As a result, a phase noise lower than the minimum offset frequency given by Eq. (9) cannot be measured.

2. Phase Noise due to ADC Clock Jitter

The ADC clock jitter also affects the phase noise of the sampled signal. To find this, the total phase $\phi_T(t)$ of $s_d(t)$ in Fig. 1 is represented by

$$\phi_T(t) = \omega_d t + \phi_d. \tag{10}$$

In Eq. (10), ω_d and ϕ_d are the frequency and phase of the SUT respectively. Note that ϕ_d randomly fluctuates. For an ADC sampling frequency $\omega_s = 2\pi f_s$, the time t_s that sampling occurs is

$$t_s = n\Delta t + \frac{\phi_c}{\omega_s}, \text{ for } n = 0,1,\cdots . \tag{11}$$

In Eq. (11), $\Delta t = 1/f_s$, and ϕ_c is the phase fluctuation caused by the phase noise of the ADC clock signal. Eq. (11) means that the sampling time t_s jitters due to the phase fluctuation ϕ_c. Thus, ϕ_A in Eq. (5a) without ϕ_1 due to the ADC clock jitter is

$$\phi_A = \phi_T(nt_s) = \omega_d(n\Delta t) + \phi_d + \frac{\omega_d\phi_c}{\omega_s}. \tag{12}$$

The last two terms ϕ_d and $\frac{\omega_d\phi_c}{\omega_s}$ in Eq. (12) represent the phase fluctuation of the SUT and the added phase fluctuation due to the ADC clock jitter. Defining the frequencies of the SUT and reference signal by ω_d and ω_{ref}, respectively, the constants *a* and *b* in Eq. (5) are given by

$$a = \frac{\omega_d}{\omega_s} \text{ and } b = \frac{\omega_{ref}}{\omega_s}. \tag{13}$$

In this paper, we propose a method to verify the relation given by Eq. (13) using the cross correlation. The phase noise due to the ADC clock jitter can be obtained by averaging the cross-power spectrum of ϕ_A and ϕ_B as follows:

$$\begin{aligned}&\langle X(\phi_A,\phi_B;f_m)\rangle_{M\to\infty}\\ &\quad= \langle R_{AB} + jI_{AB}\rangle_{M\to\infty} = abS_{\phi_c}(f_m).\end{aligned} \tag{14}$$

Similarly, averaging the cross-power spectrum of ϕ_A and ϕ_C

$$\begin{aligned}&\langle X(\phi_A,\phi_C;f_m)\rangle_{M\to\infty}\\ &\quad= \langle R_{AC} + jI_{AC}\rangle_{M\to\infty}\\ &\quad= S_{\phi_d}(f_m) + a^2S_{\phi_c}(f_m) \cong a^2S_{\phi_c}(f_m).\end{aligned} \tag{15}$$

In Eq. (15), $S_{\phi_d}(f_m)$ is the SUT phase spectrum. When the SUT with a low phase noise is selected, $\langle X(\phi_A,\phi_C;f_m)\rangle_{M\to\infty}$ can be approximated by $a^2S_{\phi_c}(f_m)$ as in Eq. (15).

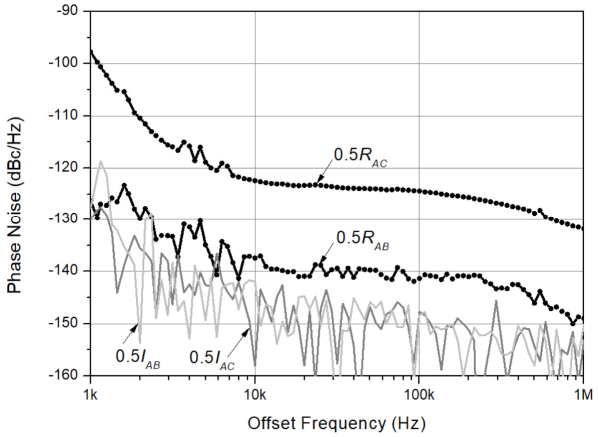

Fig. 5. The averaged cross spectrums of $X(\phi_A,\phi_B;f_m) = R_{AB} + jI_{AB}$ and $X(\phi_A,\phi_C;f_m) = R_{AC} + jI_{AC}$ in Eqs. (14) and (15). The SUT and reference signal frequencies are 1.4151 GHz and 50 MHz, respectively. The average number is $M = 10{,}000$, and the sampling frequency is $f_s = 200$ MHz.

Fig. 5 shows R_{AB} and R_{AC} in Eqs. (14) and (15). The SUT and reference signal frequencies are 1.4151 GHz and 50 MHz, respectively. The synthesized signal generator E8257D [24] is used as the SUT signal, and 50 MHz OCXO from Wenzel Associates [25] is used as the reference signal. The sampling frequency is set to $f_s = 200$ MHz, and the average number is set to $M = 10{,}000$. In Fig. 5, it can be found that the approximation holds because $R_{AC} = a^2S_{\phi_c}(f_m)$ is sufficiently larger than $S_{\phi_c}(f_m)$, the phase noise of 1.4151 GHz signal given in the datasheet.

From R_{AB} and R_{AC} in Eqs. (14) and (15), they have the same frequency dependence. Note that the frequency dependence of R_{AC} and R_{AB} on f_m in Fig. 5 are found to be almost equal. Their ratio should be b/a = (50 MHz /1.4151 GHz)$^{-1}$ = $(28.3)^{-1} = -14.5$ dB. To confirm b/a, the phase noise values are read from Fig. 5 at $f_m = 10$ kHz. The phase noise values are -122.3 dBc/Hz and -137.4 dBc/Hz, respectively, and the difference is about -15.1 dB, which is close to the predicted value of $b/a = -14.5$ dB.

In the case of R_{AB}, M should be sufficiently increased to attenuate the uncorrelated components in ϕ_A and ϕ_B. For $f_s = 200$ MHz, the phase noise floor due to the ADC phase fluctuation is about -124.5 dBc/Hz, as explained in Section III-1. The proper average number M is estimated to be more than 10^5 to measure the phase noise of about -150 dBc/Hz. Consequently, the imaginary part of the cross-power spectrum is not sufficiently suppressed as shown in Fig. 5, and R_{AB} shows a significant fluctuation.

IV. SUT PHASE NOISE EXTRACTION

As explained in Section III, the SUT phase noise can be

determined by removing the added ADC phase noises in Eq. (5). However, the removal is not simple, and the removal method was first proposed in [10]. Fig. 6 shows the block diagram of the method presented in [10]. As a result, they achieved the digital phase noise measurement system with a phase noise floor about −170 dBc/Hz for the frequency range of 1–30 MHz. Based on the technique in [10], a digital phase/amplitude modulation (PM/AM) noise measurement system [11] and a full digital phase noise measurement system [12] have been developed. To explain the pros and cons of our method, comparing it with the method in [10], which we refer to as the traditional method, is necessary.

There may be several methods other than those shown in Fig. 6 to extract the SUT phase noise. When comparing the various methods, the question is about the properties of the cross-correlated output like $S_A(f_m)$ in Fig. 6 and about the phase noise floor levels of ϕ_α and ϕ_β that are used to obtain the cross-correlated output. Note that the phase noise floor levels of ϕ_α and ϕ_β are different from those of ϕ_A, ϕ_B, ϕ_C, and ϕ_D as a result of the operation. Whether or not $S_A(f_m)$ contains phase noises other than the SUT phase noise should be investigated because the phase noise contributions of the other phase noises should be subtracted to obtain the true SUT phase noise from $S_A(f_m)$. In addition, as explained in Section III-1, the phase noise floor levels of ϕ_α and ϕ_β determine the measurable phase noise range. In this paper, the theoretical investigation on cross-correlated outputs and phase noise floor levels is presented. Based on the investigation, we propose a novel cross-correlation method for extracting the SUT phase noise.

1. Traditional Method

From Fig. 6, ϕ_α and ϕ_β are given by

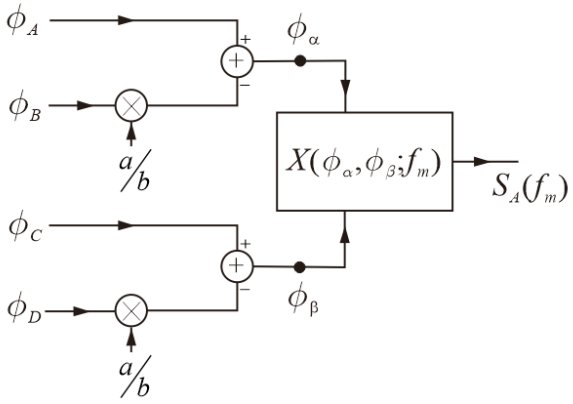

Fig. 6. The technique of the ADC clock jitter removal and the suppression of the phase noise floors in [10]. The ADC clock jitter does not appear at ϕ_α and ϕ_β. The cross-correlation operation suppresses the uncorrelated parts of ϕ_α and ϕ_β and produces $S_A(f_m)$.

$$\phi_\alpha = \phi_d - \frac{a}{b}\phi_{ref} + \phi_1 - \frac{a}{b}\phi_2 = \phi_d - \frac{a}{b}\phi_{ref} + U_A \quad (16a)$$

$$\phi_\beta = \phi_d - \frac{a}{b}\phi_{ref} + \phi_3 - \frac{a}{b}\phi_4 = \phi_d - \frac{a}{b}\phi_{ref} + V_A. \quad (16b)$$

As shown in Eq. (16), the correlated term is $\phi_d - (a\phi_{ref})/b$, while U_A and V_A are uncorrelated. Therefore, the phase spectrum $S_A(f_m)$ in Fig. 6 obtained from $\langle X(\phi_\alpha, \phi_\beta; f_m)\rangle_{M\to\infty}$ is

$$S_A(f_m) = S_{\phi_d}(f_m) + \frac{a^2}{b^2}S_{\phi_{ref}}(f_m). \quad (17)$$

Notably, $S_A(f_m)$ in Eq. (17) includes the reference signal phase noise scaled by $\frac{a^2}{b^2}$. Therefore, to determine the SUT phase noise using $S_A(f_m)$, the reference signal phase noise should be sufficiently low. Reflecting the reference signal phase noise effect on $S_A(f_m)$, a low phase noise signal source like a 100-MHz low phase noise OCXO should be selected. The frequency of such a reference signal is usually fixed and not variable. The state-of-the-art phase noise is about −180 dBc/Hz.

In addition, the phase noise floor for $S_A(f_m)$ is determined by the cross correlation of U_A and V_A. From U_A and V_A in Eq. (16), the thermal phase noise floors are $\phi_1 - (a\phi_2)/b$ and $\phi_3 - (a\phi_4)/b$. Thus, the cross correlation of U_A and V_A for the average number of M is

$$\langle X(U_A, V_A; f_m)\rangle_M = \sqrt{\frac{1}{M}\left\{1 + \left(\frac{a}{b}\right)^2\right\}}P_\phi(f_s) \quad (18)$$

where $P_\phi(f_s)$ is the phase noise floor value of ϕ_j (j = 1, 2, 3, and 4) explained in Section III-1. It should be noted that the phase noise floor rises from $P_\phi(f_s)$ by the factor $1 + \left(\frac{a}{b}\right)^2$. Consequently, the measurable phase noise range is reduced by the factor $1 + \left(\frac{a}{b}\right)^2$ from $P_\phi(f_s)$.

In case that the SUT's frequency is lower than the reference signal's frequency, the factor (a/b) is small and the rising factor $1 + \left(\frac{a}{b}\right)^2$ is negligible. However, if (a/b) is significantly large, which means that the SUT frequency is higher than the reference signal frequency, the measurable phase noise range explained in Section III-1 is significantly reduced due to the phase noise floor rise from $P_\phi(f_s)$ in Eq. (18), and the SUT with a low phase noise cannot be measured.

2. Proposed Cross-Correlation Method

Fig. 7 shows the proposed method. In Fig. 7, ϕ_A and ϕ_γ are given by

$$\phi_A = \phi_d + a\phi_c + \phi_1 = \phi_d + U_B \quad (19a)$$

$$\phi_\gamma = \phi_d - \frac{a}{b}\phi_{ref} + \phi_3 - \frac{a}{b}\phi_2 = \phi_d + V_B. \quad (19b)$$

From (19a) and (19b), the only correlated term is ϕ_d.

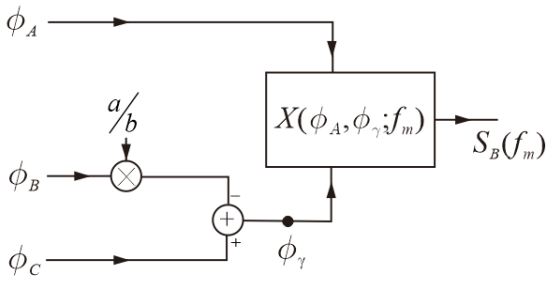

Fig. 7. The proposed technique of the ADC clock jitter removal involves the suppression of the uncorrelated parts of ϕ_A and ϕ_γ.

Note that U_B and V_B are uncorrelated. Therefore, $S_B(f_m) = \langle X(\phi_A, \phi_\gamma; f_m)\rangle_{M\to\infty}$ is given by

$$S_B(f_m) = S_{\phi_d}(f_m) \tag{20}$$

In contrast to $S_A(f_m)$ in Eq. (17), $S_B(f_m)$ does not contain the reference signal phase noise. Similarly, the phase noise floor for $S_B(f_m)$ is determined by the cross correlation of U_B and V_B. Note that U_B at higher fm is determined by ϕ_1 because $a\phi_c$ rapidly decreases as fm increases, and V_B at higher fm is determined by $\phi_3 - (a\phi_2)/b$. The phase noise floor for $S_B(f_m)$ is determined by

$$\langle X(U_B, V_B; f_m)\rangle_M = \sqrt{\frac{1}{M}\left\{1 + \left(\frac{a}{b}\right)^2\right\}^{\frac{1}{2}}} P_\phi(f_s). \tag{21}$$

The comparison of the traditional and proposed phase noise measurement methods from Eqs. (16) to (21) is summarized in Table 1.

It is important that $S_B(f_m)$ in Eq. (20) does not contain the reference signal phase noise. The $S_B(f_m)$ in Eq. (20) makes it possible to obtain the SUT phase noise from $S_B(f_m)$ even if the reference signal phase noise is not sufficiently low or if it is comparable to the SUT phase noise. In such a condition, the variable frequency signal generator with an appropriate phase noise can be chosen for the reference signal instead of a fixed frequency oscillator with an ultra-low phase noise like OCXO. Because the frequency of the reference signal generator can be freely chosen, the factor (a/b) can be made arbitrarily small. Consequently, the measurable phase noise range explained in Section III-1 can be preserved, and the phase noise of the SUT within the measurable phase noise range can be measured. In contrast, in the traditional method, the factor (a/b) is fixed, and the measurable phase noise range may be significantly reduced for a high frequency SUT.

Table 1. Comparison of the traditional and proposed phase noise measurement methods

Method	Added reference signal phase noise	Phase noise floor rise from $P_\phi(f_s)$ (dB)
Traditional	$a^2 S_{ref}(f_m)/b^2$	$10\log(1 + a^2/b^2)$
Proposed	0	$5\log(1 + a^2/b^2)$

V. Measured Phase Noises

1. Synthesized Signal Generator E8257D

The first SUT is the synthesized signal generator E8257D [24], and its phase noise is measured using the proposed phase noise measurement method. The frequency and power are set to 1.4151 GHz and 5 dBm, respectively. First, the phase noise of E8257D is measured using the signal source analyzer E5052B. The phase noise measured by E5052B at $f_m = 10$ MHz is about −149 dBc/Hz.

The phase noise of E8257D was measured using the proposed phase noise measurement method. The sampling frequency $f_s = 8$ GHz is selected. The phase noise floor is about −136 dBc/Hz, and it will be lowered to about −156 dBc/Hz for $M = 10{,}000$ (Fig. 8). Due to higher $f_s = 8$ GHz, the phase noise at lower f_m cannot be measured. The minimum offset frequency is set to $f_{m,min} = 8$ kHz from Eq. (9). The frequency of the reference signal is selected as $f_{ref} = 2.41$ GHz. The reference signal is provided using the synthesized signal generator E4438C [26] from Keysight Technologies. The E4438C phase noise at 2.41 GHz is measured by E5052B, and it is higher by about 5 dB below $f_m = 1$ MHz than the E8257D phase noise. From $f_{ref} = 2.41$ GHz, $a/b = \omega_d/\omega_{ref} = 0.587$. The phase noise floor rise is about $10\log\sqrt{1 + 0.587^2} = 0.64$ dB. Therefore, the phase noise floor rise can be neglected.

For $f_s = 8$ GHz and $f_{ref} = 2.41$ GHz, the measured phase noise of E8257D for $M = 10{,}000$ is compared in Fig. 8, and it

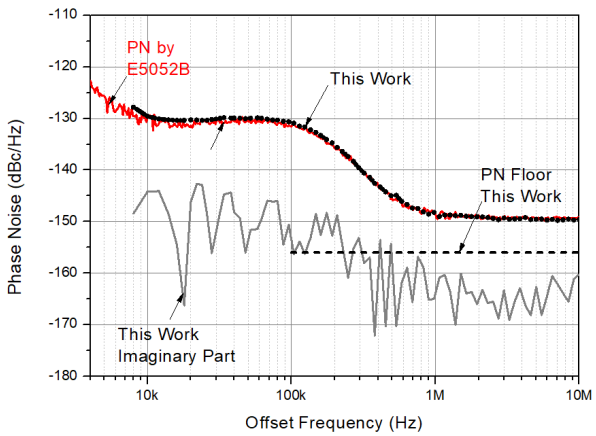

Fig. 8. The measured phase noise of E8257D from Keysight Technologies using the proposed phase noise measurement method for $M = 10{,}000$. The frequency and power of E8257D are 1.4151 GHz and 5 dBm, respectively. The reference signal frequency 2.41 GHz is provided using E4438C from Keysight Technologies.

shows remarkable agreement with that measured by E5052B. The imaginary part is also shown in Fig. 8, which is about 10 dB lower than the real part. Therefore, the uncorrelated noise is found to be sufficiently attenuated compared with the correlated noises.

To compare the proposed and traditional methods, the phase noise of E8257D is measured again using the traditional method. In the traditional method, the reference signal is the 50 MHz OCXO from Wenzel Associates [25], and its phase noise is shown in Fig. 9. The phase noise of Wenzel OCXO is measured using R&S FSPN, and it is about −184 dBc/Hz at $f_m = 100$ kHz. The measured phase noise for $f_s = 8$ GHz using the traditional method shows a significant gap with that measured by E5052B. Even the measured phase noise for $f_s = 16$ GHz, which is the maximum sampling frequency of MXR608A for the lower phase noise floor, shows a significant gap.

This is because the phase noise floor rise is quite high to measure the phase noise of E8257D. Due to the significant phase noise floor rise, it can be seen that the two-phase noises measured using the traditional methods show a significant gap. For the selected 50 MHz reference signal, the phase noise floor rise and the added reference phase noise between the proposed and traditional methods are compared in Table 2.

From Table 2, the reference phase noise in $S_A(f_m)$ is −155 dBc/Hz and the reference signal phase noise in $S_A(f_m)$ can be neglected. However, the phase noise floor rise is 29 dB, and the resulting phase noise floor at $f_s = 8$ GHz and $M = 10{,}000$ is about −127 dBc/Hz, which is quite high for measuring the SUT phase noise having a value of about −150 dBc/Hz. Even the improved phase noise floor obtained by altering $f_s = 16$ GHz and $M = 10{,}000$ is −130 dBc/Hz, which is still high for

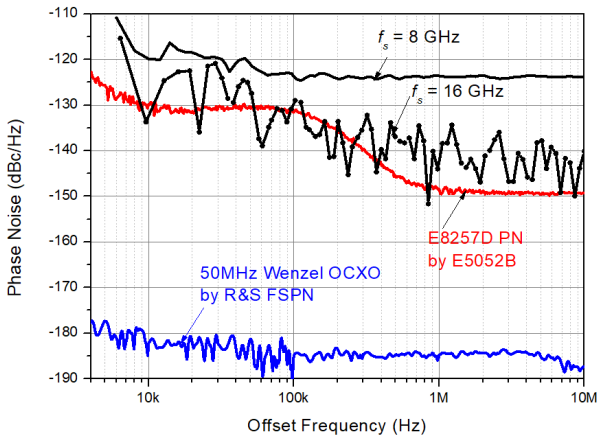

Fig. 9. Comparison of the phase noise of E8257D measured using the traditional phase noise measurement method with that measured by E5052B. The frequency and power of E8257D are 1.4151 GHz and 5 dBm, respectively. The average number for $M = 10{,}000$, and the reference signal is 50 MHz Wenzel OCXO.

Table 2. Comparison of the traditional and proposed phase noise measurement methods for E8257D

	Method	
	Traditional	Proposed
Reference signal		
Frequency	50 MHz	2.41 GHz
Phase noise (dBc/Hz) at $f_m = 100$ kHz	−184	−127
Phase noise floor rise from $P_\phi(f_s)$	29 dB	0.64 dB
Added reference signal phase noise (dBc/Hz)	−184 + 29 = −155	0

measuring the SUT phase noise. Thus, due to the significant phase noise floor rise, the correct value of the SUT phase noise cannot be measured.

From Fig. 9, we can conclude that the correct SUT phase noise cannot be measured using the traditional method when the SUT frequency is higher than the reference signal frequency. A higher SUT frequency generates a higher phase noise floor. Consequently, the measurement of the correct phase noise for a higher-frequency SUT is not possible. It should be noted that the traditional method raises the phase noise floor in the course of the ADC jitter removal. Note that the phase noise floor of the digital oscilloscope is sufficiently low. In contrast, the proposed method almost preserves the phase noise floor of the digital oscilloscope, and the phase noise of E8257D can be successfully measured.

2. Function Generator 33600A

The second SUT is the function generator 33600A [27] from Keysight Technologies. The frequency and power are set to 49.1 MHz and 5 dBm, respectively. This is the case when the SUT frequency is close to the reference signal frequency. The phase noise of 33600A is measured using E5052B (Fig. 10). The phase noise at a frequency offset of 1 MHz is about −146 dBc/Hz.

To measure the phase noise using the proposed method, the sampling frequency $f_s = 4$ GHz is selected. The phase noise floor for $M = 10{,}000$ is about −153 dBc/Hz, which is low enough to measure the phase noise of 33600A with −146 dBc/Hz. The signal generator E8257D is used for the reference signal, and its frequency is set to 1.4151 GHz. For the selected reference signal, the phase noise floor rise and the added reference signal phase noise are computed in Table 3. From the table, it can be seen that the phase noise floor rise for the proposed method is negligible. The measured SUT phase noise using the proposed method for $M = 10{,}000$ is shown and compared in Fig. 10. The measured phase noise using the proposed method shows re-

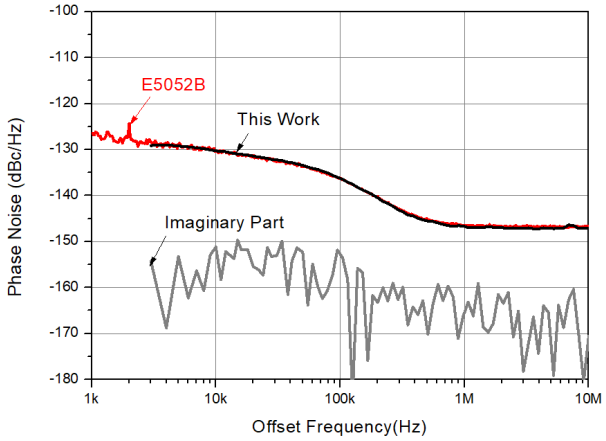

Fig. 10. The comparison of the phase noises of the function generator 33600A measured by the proposed method for M = 10,000 and by E5052B. The frequency and power of 33600A are 49.1 MHz and 5 dBm, respectively. The reference signal frequency is set to 1.4151 GHz, and the sampling frequency f_s = 4 GHz.

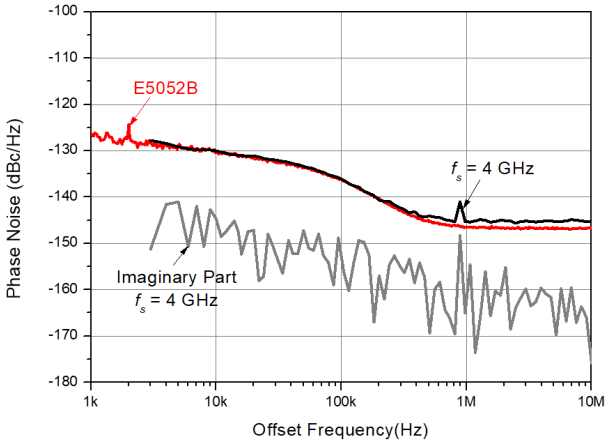

Fig. 11. The phase noises of the function generator 33600A measured using the traditional method for M = 10,000 and Keysight E5052B. The frequency and power of 33600A are 49.1 MHz and 5 dBm, respectively. In the traditional method, the reference signal is the 50 MHz OCXO from Wenzel Associates.

markable agreement with that measured by E5052B. The imaginary part of this work is shown in Fig. 10, which is about 10 dB lower compared with the real part.

The phase noise of 33600A is measured again using the traditional method. The 50 MHz OCXO from Wenzel Associates is the reference signal for the traditional method. The same sampling frequency f_s = 4 GHz as the proposed method is used. For the 50 MHz reference signal, the phase noise floor rise and the added reference signal phase noise are computed and shown in Table 3.

From Table 3, it can be seen that the 50 MHz reference signal adds a negligible reference signal phase noise to $S_A(f_m)$, and the SUT phase noise can be directly determined from $S_A(f_m)$. However, the phase noise floor rises by about 3 dB, and the resulting phase noise floor is about −150 dBc/Hz. The phase noise floor −150 dBc/Hz is close to the SUT phase noise −146 dBc/Hz. Fig. 11 shows the measured phase noises using the traditional method for f_s = 4 GHz. It can be seen that the measured phase noise using the traditional method shows a close agreement with a lower f_m, but it shows the gap at far out f_m. The gap of 1.5 dB at a higher f_m is due to the phase noise floor rise. Therefore, we can find that the traditional method yields the SUT phase noise close to the correct one for the SUT whose frequency is lower than the reference signal frequency. However, the method shows a significant gap for a higher-frequency SUT.

Table 3. Comparison of the traditional and proposed phase noise measurement methods for 33600A

	Method	
	Traditional	Proposed
Reference signal		
Frequency	50 MHz	1.4151 GHz
Phase noise (dBc/Hz) at f_m = 100 kHz	−184	−132
Phase noise floor rise from $P_\phi(f_s)$	2.9 dB	2.4×10^{-4} dB
Added reference signal phase noise (dBc/Hz)	−184 − 0.15 = −184.2	0

3. Phase Noise Floor

The Wenzel 50 MHz OCXO was selected as the third SUT. The E8257D is used as the reference signal, and its frequency was set to 1.4151 GHz. The phase noise of the Wenzel 50 MHz OCXO is about −180 dBc/Hz as shown in Fig. 9. Therefore, the sampling frequency is set to f_s = 16 GHz for the lowest phase noise floor. According to Section III-1, when f_s = 16 GHz and M = 10,000, the phase noise floor is estimated to be about −160 dBc/Hz, which is the lowest phase noise floor value.

Taking the phase noise value of about −160 dBc/Hz into consideration, the phase noise of the SUT, the Wenzel 50 MHz OCXO cannot be measured. The measured phase is inferred to show the phase noise floor value of −160 dBc/Hz. The measured phase noise of the Wenzel 50 MHz OCXO is shown in Fig. 12. As expected, it can be seen that it has a phase noise of about −160 dBc/Hz above f_m = 100 kHz. The measurement in Fig. 12 provides a way of measuring the phase noise floor value or the sensitivity of the phase noise measurement system. In other words, the system phase noise floor can be alternatively determined by measuring the phase noise of the SUT whose phase

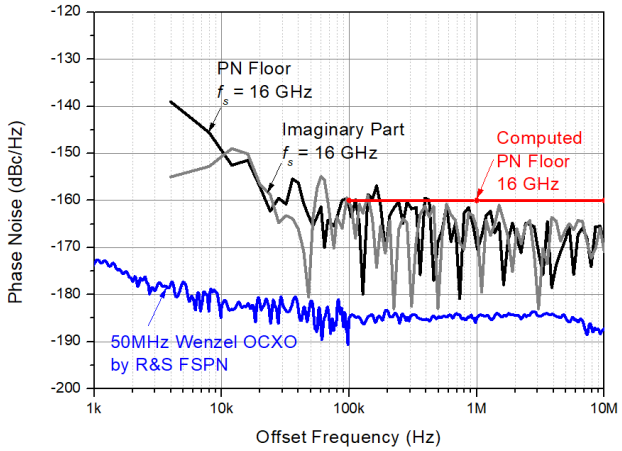

Fig. 12. The phase noise of the Wenzel 50 MHz OCXO measured using the proposed method. The E8257D is used as the reference signal, and its frequency is set to 1.4151 GHz.

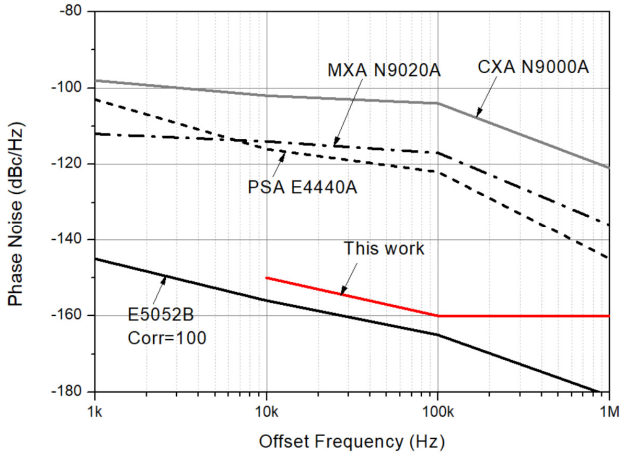

Fig. 13. The phase noise floors of this work, the various spectrum analyzers, and SSA E5052B for the number of correlation (=100). The spectrum analyzer phase noise floors are plotted using typical values, and option 503, 507 are assumed for the spectrum analyzers.

noise is below its phase noise floor value instead of the analysis explained in Section III-1. Therefore, the phase noise floor of the phase noise measurement system in this paper is about −160 dBc/Hz.

VI. Conclusion

In this paper, we proposed a phase noise measurement method using a 10-bit digital oscilloscope MXR608A from Keysight Technologies. In addition, we analyzed the ADC phase noise floors and the phase noise due to ADC clock jitter. To evaluate the proposed phase noise measurement method, the phase noises of the synthesized signal generator E8257D and the function generator 33600A from Keysight Technologies were measured. The phase noises measured using the proposed phase noise measurement method were compared with those measured using E5052B. The measured phase noises using the proposed phase shows close agreements with those measured with E5052B.

To assess the proposed phase noise measurement method, the phase noise floors of the various general-purpose spectrum analyzers [28] and E5052B for the number of correlation (=100) are shown in Fig. 13. In the case of the spectrum analyzers, typical values instead of specification values were employed to plot. In addition, the phase noise floor of this work was shown for comparison. As shown in Fig. 13, the phase noise floor of this work is far below those of the spectrum analyzers. Therefore, although the phase noise floor of the proposed technique still does not reach that of E5052B, it can be used to measure the phase noise of various SUTs below the phase noise floors of general-purpose spectrum analyzers.

Table 4 compares this work with other works on digital phase noise measurements. Although the number of the ADC bits of this work is smaller compared with other works (phase noise floor degradation of about 20 dB more), the phase noise floor is comparable or better. In particular, the bandwidth is wider than any other works, which is advantageous as a phase noise measurement equipment. We believe that the proposed method is valuable when considering future advances in the number of ADC bits and the bandwidth of digital oscilloscope hardware.

Table 4. Comparison of this work with other digital phase noise measurements

	Grove et al. [10]	Imaike [13]	D'Arco and de Vito [14]	This work
Oscilloscope	No	No	Yes	Yes
ADC bits	14–15	16	8	10
Bandwidth (MHz)	1–30	15[a]	6,000	6,000
Hardware	ADC, FPGA	Data capture	-	Data capture
Clock phase noise compensation	Yes	No	No	Yes
Phase noise floor (dBc/Hz)	−173	−155	−106	−160[b]

[a]Bandpass filter of 15 MHz bandwidth is employed.
[b]f_s = 16 GHz, M = 10,000.

This work was supported by research fund of Chungnam National University.

References

[1] *IEEE Standard Definitions of Physical Quantities for Fundamental Frequency and Time Metrology - Random Instabilitie*s, IEEE Standard 1139-2008, 2008.

[2] Y. Jeon, J. Koo, and H. Kim, "Design of a Ka band multichannel (25CH) millimeter-wave downconverter for a signal intelligence system," *Journal of Electromagnetic Engineering and Science*, vol. 19, no. 3, pp. 210-219, 2019.

[3] Y. Jeon and S. Bang, "Front-end module of 18-40 GHz ultra-wideband receiver for electronic warfare system," *Journal of Electromagnetic Engineering and Science*, vol. 18, no. 3, pp. 188-198, 2018.

[4] B. J. Jang, H. G. Yoon, and J. B. Lim, "Hardware design and deployment issues in UHF RFID systems," *Journal of Electromagnetic Engineering and Science*, vol. 9, no. 1, pp. 39-45, 2009.

[5] U. L. Rohde, A. K. Poddar, and A. M. Apte, "Getting its measure: oscillator phase noise measurement techniques and limitations," *IEEE Microwave Magazine*, vol. 14, no. 6, pp. 73-86, 2013.

[6] A. K. Poddar, U. L. Rohde, and A. M. Apte, "How low can they go? Oscillator phase noise model, theoretical, experimental validation, and phase noise measurements," *IEEE Microwave Magazine*, vol. 14, no. 6, pp. 50-72, 2013.

[7] Rohde & Schwarz, "R&S FSPN phase noise analyzer and VCO tester user manual," 2021 [Online]. Available: https://www.rohde-schwarz.com/cz/manual/r-s-fspn-user-manual-manuals-gb1_78701-1129408.html.

[8] Keysight Technologies, "E5052B Signal Source Analyzer datasheet: 10 MHz to 7 GHz, 26.5 GHz, or 110 GHz," 2022 [Online]. Available: https://www.keysight.com/us/en/assets/7018-01528/data-sheets/5989-6388.pdf.

[9] L. Angrisani, M. D'Apuzzo, and M. D'Arco, "A digital signal-processing approach for phase noise measurement," *IEEE Transactions on Instrumentation and Measurement*, vol. 50, no. 4, pp. 930-935, 2001.

[10] J. Grove, J. Hein, J. Retta, P. Schweiger, W. Solbrig, and S. R. Stein, "Direct-digital phase-noise measurement," in *Proceedings of the 2004 IEEE International Frequency Control Symposium and Exposition*, Montreal, Canada, 2004, pp. 287-291.

[11] C. W. Nelson and D. A. Howe, "A sub-sampling digital PM/AM noise measurement system," in *Proceedings of 2012 IEEE International Frequency Control Symposium Proceedings*, Baltimore, MD, 2012, pp. 1-4.

[12] L. B. Ruppalt, D. R. McKinstry, K. C. Lauritzen, A. K. Wu, S. A. Phillips, and S. H. Talisa, "Simultaneous digital measurement of phase and amplitude noise," in *Proceedings of 2010 IEEE International Frequency Control Symposium*, Newport Beach, CA, 2010, pp. 97-102.

[13] T. Imaike, "Full digital phase noise measurement by using two reference oscillators and multichannel ADCs," in *Proceedings of 2017 Joint Conference of the European Frequency and Time Forum and IEEE International Frequency Control Symposium (EFTF/IFCS)*, Besancon, France, 2017, pp. 583-586.

[14] M. D'Arco and L. De Vito, "A novel method for phase noise measurement based on cyclic complementary autocorrelation," *IEEE Transactions on Instrumentation and Measurement*, vol. 65, no. 12, pp. 2685-2692, 2016.

[15] Keysight Technologies, "Infiniium MXR-Series datasheet," 2022 [Online]. Available: https://www.keysight.com/us/en/assets/7120-1115/data-sheets/Infiniium-MXR-Series.pdf.

[16] J. E. Volder, "The CORDIC trigonometric computing technique," *IRE Transactions on Electronic Computers*, vol. 8, no. 3, pp. 330-334, 1959.

[17] Wikipedia, "CORDIC," 2021 [Online]. Available: https://en.wikipedia.org/w/index.php?Title=CORDIC&oldid=1026743048.

[18] National Instruments, "Understanding FFTs and Windowing," 2021 [Online]. Available: https://download.ni.com/evaluation/pxi/Understanding%20FFTs%20and%20Windowing.pdf.

[19] P. Fleischmann, H. Mathis, J. Kucera, and S. Dahinden, "Implementation of a cross-spectrum FFT analyzer for a phase-noise test system in a low-cost FPGA," *International Journal of Microwave Science and Technology*, vol. 2015, article no. 757591, 2015. https://doi.org/10.1155/2015/757591

[20] P. Welch, "The use of fast Fourier transform for the estimation of power spectra: a method based on time averaging over short, modified periodograms," *IEEE Transactions on Audio and Electroacoustics*, vol. 15, no. 2, pp. 70-73, 1967.

[21] J. C. Brown, "Calculation of a constant Q spectral transform," *The Journal of the Acoustical Society of America*, vol. 89, no. 1, pp. 425-434, 1991.

[22] W. Kester, "Fundamentals of sampled data systems," in Analog-Digital Conversion. Wilmington, MA: Analog Devices Inc., 2004.

[23] E. Rubiola and F. Vernotte, "The cross-spectrum experimental method," 2018 [Online]. Available: https://arxiv.org/abs/1003.0113.

[24] Keysight Technologies, "E8257D PSG microwave analog signal generator datasheet," 2022 [Online]. Available: https://www.keysight.com/us/en/product/E8257D/psg-analog-signal-generator-100-khz-67-ghz.html.

[25] Wenzel Associates Inc., "Product model: VHF UL," 2021 [Online]. Available: https://wenzel.com/model/vhf-uln/.

[26] Keysight Technologies, "E4428C & E4438C ESG signal generators user's guide," 2022 [Online]. https://www.keysight.com/us/en/assets/9018-01484/user-manuals/9018-01484.pdf.
[27] Keysight Technologies, "33500B and 33600A series trueform waveform generators datasheet," [Online]. Available: https://www.keysight.com/us/en/assets/7018-05928/data-sheets/5992-2572.pdf.
[28] Keysight Technologies, "Keysight N9000A CXA signal analyzer," 2018 [Online]. Available: https://www.keysight.com/us/en/assets/9018-04769/technical-specifications/9018-04769.pdf.

Kyung-Whan Yeom

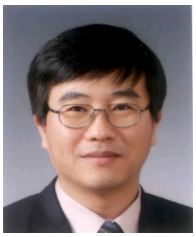

was born in Seoul, South Korea, in 1957. He received the B.S. degree in electronics from Seoul National University, Seoul, in 1980, and the M.S. and Ph.D. degrees in electrical engineering from the Korea Advanced Institute of Science and Technology, Daejeon, South Korea, in 1982 and 1988, respectively. From 1985 to 1991, he was a Principal Engineer with LG Precision, Anyang, where he was a Team Leader with the Microwave Integrated Circuit Team and was subsequently involved in the Military Electronics Division for electronic warfare equipment. From 1991 to 1995, he was with LTI, Seoul, where he was involved in power-amplifier modules for analog cellular phones. In 1995, he joined Chungnam National University, Daejeon, as an Assistant Professor, where he is currently a Professor with the Department of Radio Science and Engineering. He has authored the book Microwave Circuit Design: A Practical Approach Using Advanced Design System. His current research interests include the design of hybrid and monolithic microwave circuits and microwave systems. Dr. Yeom is the member of the Korean Institute of Electromagnetic Engineering and Science (KIEES) since 1995. He was the Editor-in-Chief of KIEES from 2004 to 2006. He received the IR-52 Jang Youg-Sil Prize from the Ministry of Science and Technology of Korea for his work on cell phone power amplifiers in 1994, the Academic Award from KIEES for "the design and fabrication of a novel 60 GHz GaAs pHEMT resistive double balanced star MMIC mixer" in 2004, and the Best Paper Award from the Korean Federation of Science and Technology Societies for his work, "a novel design method of direct coupled bandpass filter based on EM simulation of individual resonator."

Jin-Seong Roh

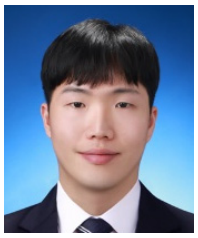

was born in Yesan, Korea, in 1995. He received the B.S. degrees in the Department of Radio Science and Engineering from the Chungnam National University, Daejeon, Korea, in 2020. He is currently working toward the M.S. degree in Radio Science and Engineering at Chungnam National University, Daejeon, Korea. His research interests are measurement methods of phase noise and design of microwave circuits and microwave systems.